Robotics and Autonomous Systems 78 (2016) 36–48

Contents lists available at ScienceDirect

Robotics and Autonomous Systems

journal homepage: www.elsevier.com/locate/robot

Robust adaptive tracking control of wheeled mobile robot

Linjie Xin [a], Qinglin Wang [a], Jinhua She [b], Yuan Li [a,*]

[a] School of Automation, Beijing Institute of Technology, Zhongguancun Street, Haidian District, Beijing, 100081, China
[b] School of Engineering, Tokyo University of Technology, 1404-1 Katakura, Hachioji, Tokyo, 192-0982, Japan

HIGHLIGHTS

- Tracking control for a wheeled mobile robot is achieved by finite-time control.
- The disturbance observer gives an accurate compensation for system uncertainty.
- Requirement of boundary information of system uncertainty can be released.

ARTICLE INFO

Article history:
Received 5 September 2015
Accepted 18 January 2016
Available online 27 January 2016

Keywords:
Finite-time control
Disturbance observer
Robust control
Wheeled mobile robot

ABSTRACT

This paper considers the problem of robust adaptive trajectory tracking control for a wheeled mobile robot (WMR). First, the trajectory tracking of the WMR is converted to a problem of the stabilization of a double integral system. Next, a continuous finite-time control method is employed to design a tracking controller. Then, a disturbance observer and an adaptive compensator are designed to cooperate with the tracking controller for dealing with system uncertainties of the WMR. Finally, a switching adaptive law is presented in combination with the boundary layer approach to attenuate the chattering in the adaptive compensator. As a result, the control system yields the ultimate boundedness of both the tracking error and the adaptive gain. Simulation results demonstrate the validity of the new method.

1. Introduction

A wheeled mobile robot (WMR) is a typical kind of nonholonomic systems. The design of a robust control system is a difficult task due to the nonlinearities and uncertainties in the system, and has been attracting a great attention [1,2].

Tracking control for a WMR not only requires a designed controller to track a prescribed orbit, but also has to robustly stabilize the closed-loop system against the system uncertainties. The existing control methods include the nonlinear control methods, artificial intelligent methods, visual servoing control, etc. The nonlinear control methods contain backstepping method [3], sliding mode control (SMC) [4–6], and finite-time control technique [7]. And the adaptive compensation is further incorporated with the above methods to make the control system more practical [8]. For example, Jiang and Nijmeijer presented a backstepping method to achieve both the local and global tracking control based on a simplified dynamic model of WMR [9]. Lee et al. solved the tracking and regulation problems simultaneously using the backstepping method [10]. Considering the system uncertainties, the backstepping control was combined with SMC and adaptive compensation [11–13]. Focusing on that the SMC method has high robustness, the tracking control for a WMR was solved by the SMC method in [14–17]. Since the finite-time control algorithm features better performance than an asymptotically converged controller does, Ou et al. presented a finite-time approach to achieve tracking control in [18]. The twisting algorithm and terminal sliding mode (TSM) method were employed in [19,20]. In [21], A.S. Al-Araji et al. designed a feedforward controller using neural networks to find reference torques. Due to the universal approximation capability of the fuzzy control, it was introduced in [13,22] to enhance the performance of traditional controllers. And the visual servoing tracking controllers were developed in [23,24]. Although the artificial intelligent methods provide new ways for tracking control of a WMR, further studies of the nonlinear control methods are still valuable.

Previous studies theoretically achieve the control objective of tracking control and thus have great significance for the control of a WMR. On the other hand, there are some problems in the existing literatures. Firstly, since the control input in an actual control system is a motor torque, it is straightforward to use a dynamic

* Corresponding author.
E-mail addresses: xinlinjie08@163.com (L. Xin), wangql@bit.edu.cn (Q. Wang), she@stf.teu.ac.jp (J. She), liyuan@bit.edu.cn (Y. Li).

http://dx.doi.org/10.1016/j.robot.2016.01.002
0921-8890/

model in the control system design [19,25]. Note that the dynamic model is ignored or simplified in [9,10,26,27]. So, the control laws are not directly applicable. Secondly, the linear SMC methods of [15–17] are about asymptotical convergence, which means that the convergence rate is at best exponential with infinite settling time. In addition, the switching gain of SMC methods is usually chosen a large value to guarantee the robustness of the closed-loop system. It results in large amplitude of the control input. Thirdly, the robustness of the finite-time control system of [18] is not studied. And the chattering problem of adaptive finite-time method of [19] is not solved, which should be considered with the boundary of adaptive gain simultaneously [28,29].

The main contribution of this study is that a robust and adaptive control scheme is presented using the finite-time algorithm of [30–32]. As the major technical breakthrough, a TSM disturbance observer and an adaptive compensator are designed for this algorithm. The disturbance observer could give a fast accurate compensation for the system uncertainties, which avoids the large conservative switching gain. Furthermore, in the case that the boundary information of system uncertainties is unknown, the adaptive compensator could enhance the robustness of the control system. Moreover, a solution is given for the chattering reduction, which simultaneously guarantees the boundedness of adaptive gain.

This paper employs a dynamic model of a WMR and takes the motor torque as the control input. First, the tracking control is transformed to the problem of finite-time stabilization of a double integral system. Then, the design of control system is divided into two parts: a tracking controller and a compensator. The former is responsible for the tracking control of a nominal plant, which is designed using the finite-time algorithm. The latter ensures the robustness of the control system against system uncertainties, which is composed by a TSM disturbance observer and an adaptive compensator. Meanwhile, the adaptive compensator is improved by using the boundary layer approach and switching adaptive law. As a result, the control system yields the ultimate boundedness of both the tracking error and adaptive gain.

The rest of this paper is organized as follows. Preliminaries are presented in Section 2. Section 3 shows the dynamic model of a WMR. The tracking problem is also transformed to the problem of stabilizing a double integral system. In Section 4, the main result of this study, the control system design, is presented. And the simulation results are shown in Section 5. Finally, some concluding remarks are given in Section 6.

2. Preliminaries

This section presents a review of the Lyapunov theorem for finite-time stability and some useful lemmas.

Theorem 1 ([30,33]). *Consider the following non-Lipschitz continuous autonomous system*

$$\dot{x} = f(x), \quad f(0) = 0,\ x \in R^n, \tag{1}$$

where $f : R^n \to R^n$ is locally Lipschitz continuous. Assume there is a C^1 function $V(x)$ defined on a neighborhood $D \subset R^n$ of the origin, such that:

(1) *$V(x)$ is positive definite;*
(2) *$\dot{V}(x) + \alpha V^{\eta}(x) \le 0,\ x \in D, \alpha > 0,\ \eta \in (0, 1)$.*

Then, System (1) is locally finite-time stable at the origin. If $D = R^n$ and $V(x)$ is also radially unbounded, then System (1) is globally finite-time stable at the origin. The settling time, which depends on the initial state $x(0) = x_0$, satisfies $T_x(x_0) \le \frac{V(x_0)^{1-\eta}}{\alpha(1-\eta)}$, for all x_0 in some open neighborhood of the origin.

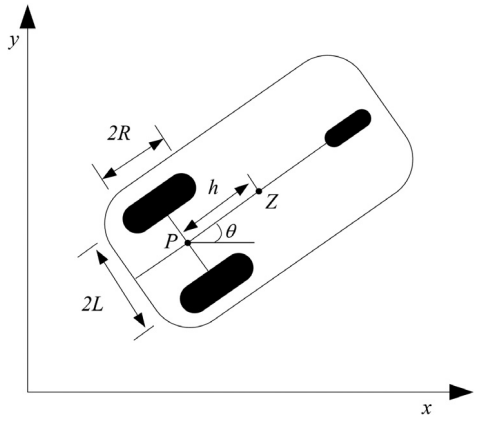

Fig. 1. Structure of WMR.

Moreover, an extended Lyapunov description of finite-time stability can be given with the form of fast TSM as

$$\dot{V}(x) + \kappa V(x) + \alpha V^{\eta}(x) \le 0, \quad \kappa > 0, \tag{2}$$

and the settling time satisfies $T \le \frac{1}{\kappa(1-\eta)} \ln \frac{\kappa V^{1-\eta}(x_0)+\alpha}{\alpha}$, where $V(x_0)$ is the initial value of $V(x)$.

Lemma 1 ([31]). *For any real numbers a_1, a_2, p_1, and p_2, if $p_1 > 0$ and $p_2 > 0$, then the following inequality holds*

$$|a_1|^{p_1} |a_2|^{p_2} \le \frac{p_1 |a_1|^{p_1+p_2}}{p_1 + p_2} + \frac{p_2 |a_2|^{p_1+p_2}}{p_1 + p_2}.$$

Lemma 2 ([32]). *For any real numbers a_3 and a_4, if $0 < p' = \frac{p_3}{p_4} < 1$, and p_3 and p_4 are positive odd integers, then*

$$\left| a_3^{p'} - a_4^{p'} \right| \le 2^{1-p'} |a_3 - a_4|^{p'}.$$

Lemma 3 ([32]). *For any real numbers c_i, $i = 1, 2, \ldots, n$ and $0 < j \le 1$, the following inequality holds*

$$(|c_1| + |c_2| + \cdots + |c_n|)^j \le |c_1|^j + |c_2|^j + \cdots + |c_n|^j.$$

3. Dynamic model of WMR

A WMR (Fig. 1) has one front castor wheel and two driving wheels. The castor wheel prevents the robot from tipping over as it moves on a plane. Two DC motors are the actuators of left and right wheels. Its dynamic equation and nonholonomic constraint are [16]

$$\begin{cases} M(\varphi)\ddot{\varphi} + C(\varphi, \dot{\varphi})\dot{\varphi} + G(\varphi) = B(\varphi)\tau + J^{\mathrm{T}}(\varphi)\lambda \\ J(\varphi)\dot{\varphi} = 0, \end{cases} \tag{3}$$

where φ denotes the pose vector, $M(\varphi)$ is a symmetric positive definite inertia matrix, $C(\varphi, \dot{\varphi})$ presents the vector of centripetal and Coriolis torques, $G(\varphi)$ is the gravitational torques, $B(\varphi)$ is the input transformation matrix, τ is the control torque, and λ is a Lagrange multiplier.

Assuming that the mobile robot moves in the horizontal plane, in this case, $G(\varphi)$ is equal to zero. The center of mass for mobile robot is located in the middle of axis connecting the rear wheels in P point as shown in Fig. 1, therefore, $C(\varphi, \dot{\varphi})$ is equal to zero [21].

Since $C(\varphi, \dot{\varphi}) = G(\varphi) = 0$, the system dynamic equation becomes

$$\begin{bmatrix} m & 0 & 0 \\ 0 & m & 0 \\ 0 & 0 & I \end{bmatrix} \begin{bmatrix} \ddot{x} \\ \ddot{y} \\ \ddot{\theta} \end{bmatrix} = \frac{1}{R} \begin{bmatrix} \cos\theta & \cos\theta \\ \sin\theta & \sin\theta \\ L & -L \end{bmatrix} \begin{bmatrix} \tau_1 \\ \tau_2 \end{bmatrix} + \begin{bmatrix} \sin\theta \\ -\cos\theta \\ 0 \end{bmatrix} \lambda, \tag{4}$$

where the pose of WMR is defined as $\varphi = (x, y, \theta)^{\mathrm{T}}$; m and I are the mass and inertia of the WMR; x and y are the position P of the center of mass; θ denotes the orientation angle of the WMR; R and $2L$ represent the radius and the distance of the driving wheels; τ_1 and τ_2 denote the torques of right and left motors, respectively.

The nonholonomic constraint, the no slip condition, is written as

$$\dot{x}\sin\theta - \dot{y}\cos\theta = 0. \tag{5}$$

The kinematic model is

$$\begin{bmatrix}\dot{x}\\ \dot{y}\\ \dot{\theta}\end{bmatrix} = \begin{bmatrix}\cos\theta & 0\\ \sin\theta & 0\\ 0 & 1\end{bmatrix}\begin{bmatrix}v\\ \omega\end{bmatrix}, \tag{6}$$

and the dynamic model is

$$\begin{bmatrix}\dot{v}\\ \dot{\omega}\end{bmatrix} = \frac{1}{R}\begin{bmatrix}1/m & 1/m\\ L/I & -L/I\end{bmatrix}\begin{bmatrix}\tau_1\\ \tau_2\end{bmatrix}, \tag{7}$$

where v and ω are the linear velocity and angular velocity, respectively.

The trajectory tracking is formulated as the problem of designing a control law to make the central position $Z(z_1, z_2)$ to track a reference trajectory $Z_d(z_{1d}, z_{2d})$.

The coordinates of Z are defined as $\begin{bmatrix}z_1\\ z_2\end{bmatrix} = \begin{bmatrix}x + h\cos\theta\\ y + h\sin\theta\end{bmatrix}$.

Let E denote the tracking error between Z and Z_d

$$E = \begin{bmatrix}e_1\\ e_2\end{bmatrix} = \begin{bmatrix}z_{1d} - z_1\\ z_{2d} - z_2\end{bmatrix}. \tag{8}$$

Calculating the second-order derivative of the tracking error along (6) gives

$$\ddot{E} = \begin{bmatrix} v\omega\sin\theta + h\omega^2\cos\theta - \dot{v}\cos\theta + h\dot{\omega}\sin\theta + \ddot{z}_{1d}\\ -v\omega\cos\theta + h\omega^2\sin\theta - \dot{v}\sin\theta - h\dot{\omega}\cos\theta + \ddot{z}_{2d}\end{bmatrix}. \tag{9}$$

For simplicity, we define $b = \begin{bmatrix} v\omega\sin\theta + h\omega^2\cos\theta + \ddot{z}_{1d}\\ -v\omega\cos\theta + h\omega^2\sin\theta + \ddot{z}_{2d}\end{bmatrix}$, $A = \frac{-1}{R}\begin{bmatrix}\cos\theta & -h\sin\theta\\ \sin\theta & h\cos\theta\end{bmatrix}\begin{bmatrix}1/m & 1/m\\ L/I & -L/I\end{bmatrix}$.

Then, (9) is rewritten as

$$\ddot{E} = b + A\tau. \tag{10}$$

However, in many cases, external disturbances and/or the changes of parameters in the operating result in system uncertainties in the modeling. Thus, we consider the following system

$$\ddot{E} = b + (A + \Delta A)(\tau + \tau_d) = U + G, \tag{11}$$

where $U = A\tau + b$ is the new control input, ΔA is the changes of parameters, τ_d denotes the external disturbances, and $G = \Delta A(\tau + \tau_d) + A\tau_d$ represents the lumped system uncertainty. It is assumed that G has a positive upper boundary $\bar{G}$. Since A is nonsingular, the actual control input is given by $\tau = A^{-1}(U - b)$. It is clear from (11) that the finite-time tracking control is equivalent to the finite-time stabilization of the following double integral system

$$\begin{cases}\dot{E}_1 = E_2\\ \dot{E}_2 = U + G.\end{cases} \tag{12}$$

4. Control system design

The structure of control system (Fig. 2) for finite-time stabilization of System (12) contains a tracking controller and a compensator.

The tracking controller is designed using the finite-time control method based on Theorem 1. It drives the states of the nominal system ($G = 0$) to the origin in a finite time. Since this control method has poor robustness, a compensator is introduced to deal with the system uncertainties. If the upper boundary $\bar{G}$ is known, a TSM disturbance observer is designed as the compensator. On the other case, an adaptive compensator is designed using the Lyapunov method. The control system design is given by the following three subsections.

4.1. Tracking controller design

Consider the following system

$$\begin{cases}\dot{x}_1 = x_2\\ \dot{x}_2 = u + G,\end{cases} \tag{13}$$

where $|G| \le \bar{G}$. Let the control input u be

$$u = u_{nom} + u_{com}, \tag{14}$$

where u_{nom} is the tracking control law, u_{com} is the compensating law.

Theorem 2. *Consider the nominal system ($G = 0$), let the control input u be*

$$u = u_{nom} = -l\varepsilon^{\frac{2-q}{q}}. \tag{15}$$

The parameters in (15) are taken as

$$\varepsilon = x_2^q - x_2^{*q}, \quad x_2^* = -ax_1^{d-1},\ a = 2^{1-\frac{1}{q}} + \mu,$$
$$l = \left(2 - \frac{1}{q}\right)a^{1+q}\left(a + 2^{2-\frac{2}{q}}\frac{1}{a}\right),\ \mu > 0,\ d = 1 + \frac{1}{q},$$
$$q = \frac{q_1}{q_2},\ 1 < q < 2,$$

where q_1 and q_2 are positive odd integers.

Then, the control law (15) stabilizes System (13) in finite time.

Proof. Define a Lyapunov function as

$$V_1 = \frac{1}{2}x_1^2. \tag{16}$$

Differentiating (16) with respect to time yields

$$\dot{V}_1 = x_1x_2 + x_1x_2^* - x_1x_2^*, \tag{17}$$

where $x_2^* = -ax_1^{d-1}$.

According to [30], a C^1 and positive definite Lyapunov function is constructed as

$$V_2 = V_1 + W \tag{18}$$

where $W = \frac{1}{\left(2-\frac{1}{q}\right)a^{1+q}}\int_{x_2^*}^{x_2}\left(s^q - x_2^{*q}\right)^{2-\frac{1}{q}}ds$. And it has the following property

$$\frac{\partial W}{\partial x_2} = \frac{1}{\left(2-\frac{1}{q}\right)a^{1+q}}\left(x_2^q - x_2^{*q}\right)^{2-\frac{1}{q}}$$
$$\frac{\partial W}{\partial x_1} = -\frac{1}{a^{1+q}}\frac{\partial\left(x_2^{*q}\right)}{\partial x_1}\int_{x_2^*}^{x_2}\left(s^q - x_2^{*q}\right)^{1-\frac{1}{q}}ds. \tag{19}$$

With $x_2^* = -ax_1^{d-1}$, differentiating (18) with respect to time for the nominal system yields

$$\dot{V}_2 = \dot{V}_1 + \dot{W} = x_1x_2 + \frac{1}{\left(2-\frac{1}{q}\right)a^{1+q}}\left(x_2^q - x_2^{*q}\right)^{2-\frac{1}{q}}\dot{x}_2$$

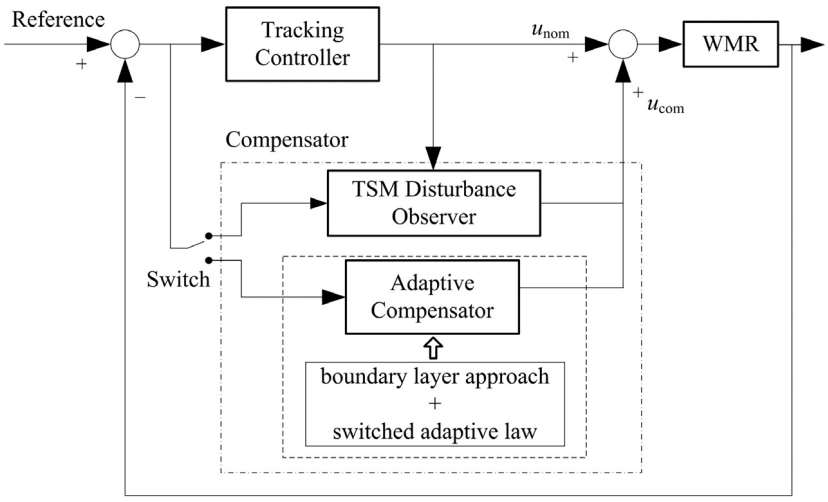

Fig. 2. Structure of the control system.

$$+\frac{1}{a}\dot{x}_1\int_{x_2^*}^{x_2}\left(s^q-x_2^{*q}\right)^{1-\frac{1}{q}}ds$$
$$=x_1x_2+x_1x_2^*-x_1x_2^*+\frac{1}{\left(2-\frac{1}{q}\right)a^{1+q}}\left(x_2^q-x_2^{*q}\right)^{2-\frac{1}{q}}u$$
$$+\frac{1}{a}x_2\int_{x_2^*}^{x_2}\left(s^q-x_2^{*q}\right)^{1-\frac{1}{q}}ds. \tag{20}$$

With $\varepsilon=x_2^q-x_2^{*q}$, we obtain

$$\dot{V}_2\le x_1x_2+x_1x_2^*-x_1x_2^*+\frac{1}{\left(2-\frac{1}{q}\right)a^{1+q}}\varepsilon^{2-\frac{1}{q}}u+\frac{1}{a}|x_2|\,\varepsilon^{1-\frac{1}{q}}\left|x_2-x_2^*\right|$$
$$\le -ax_1^d+\left|x_1x_2-x_1x_2^*\right|+\frac{1}{\left(2-\frac{1}{q}\right)a^{1+q}}\varepsilon^{2-\frac{1}{q}}u$$
$$+\frac{1}{a}|x_2|\,\varepsilon^{1-\frac{1}{q}}\left|x_2-x_2^*\right|. \tag{21}$$

It is clear from Lemmas 1 and 2 that the following holds

$$\left|x_1x_2-x_1x_2^*\right|\le 2^{1-\frac{1}{q}}|\varepsilon|^{\frac{1}{q}}|x_1|\le 2^{1-\frac{1}{q}}\left(\frac{qx_1^d}{1+q}+\frac{\varepsilon^d}{1+q}\right),$$
$$|x_2|\left|x_2-x_2^*\right|\le\left|x_2-x_2^*\right|\left|x_2-x_2^*\right|+\left|x_2^*\right|\left|x_2-x_2^*\right|$$
$$\left|x_2-x_2^*\right|\left|x_2-x_2^*\right|\le 2^{2-\frac{2}{q}}\varepsilon^{\frac{2}{q}},\quad \left|x_2^*\right|\left|x_2-x_2^*\right|\le a2^{1-\frac{1}{q}}|x_1|^{\frac{1}{q}}|\varepsilon|^{\frac{1}{q}}.$$

So (21) turns to

$$\dot{V}_2\le -ax_1^d+2^{1-\frac{1}{q}}\left(\frac{qx_1^d}{1+q}+\frac{\varepsilon^d}{1+q}\right)+\frac{1}{\left(2-\frac{1}{q}\right)a^{1+q}}\varepsilon^{2-\frac{1}{q}}u$$
$$+\frac{1}{a}2^{2-\frac{2}{q}}\varepsilon^d+2^{1-\frac{1}{q}}\left(\frac{x_1^d}{1+q}+\frac{q\varepsilon^d}{1+q}\right)$$
$$=-\left(a-2^{1-\frac{1}{q}}\right)x_1^d+\left(2^{1-\frac{1}{q}}+2^{2-\frac{2}{q}}\frac{1}{a}\right)\varepsilon^d$$
$$+\frac{1}{\left(2-\frac{1}{q}\right)a^{1+q}}\varepsilon^{2-\frac{1}{q}}u. \tag{22}$$

Substituting u_{nom} in (15) into (22), we obtain $\dot{V}_2\le-\mu x_1^d-\mu\varepsilon^d$.

From (18) and Lemma 2, for the nominal system,

$$V_2\le\frac{1}{2}x_1^2+\frac{1}{\left(2-\frac{1}{q}\right)a^{1+q}}\left|x_2-x_2^*\right||\varepsilon|^{2-\frac{1}{q}}$$
$$\le\frac{1}{2}x_1^2+\frac{2^{1-\frac{1}{q}}}{\left(2-\frac{1}{q}\right)a^{1+q}}\varepsilon^2. \tag{23}$$

Letting $\chi=\max\left\{\frac{1}{2},\frac{2^{1-1/q}}{\left(2-\frac{1}{q}\right)a^{1+q}}\right\}$ gives $V_2\le\chi x_1^2+\chi\varepsilon^2$. Letting $\alpha=\frac{\mu}{2\chi^\eta}$ and $\eta=\frac{d}{2}$, and applying Lemma 3 give

$$\dot{V}_2+\alpha V_2^\eta\le-\mu x_1^d-\mu\varepsilon^d+\frac{\mu}{2\chi^\eta}(\chi x_1^2+\chi\varepsilon^2)^{\frac{d}{2}}$$
$$\le-\frac{\mu}{2}x_1^d-\frac{\mu}{2}\varepsilon^d. \tag{24}$$

As $d=(q_1+q_2)/q_1$, and q_1 and q_2 are positive odd integers, Theorem 1 ensures that the nominal system is finite-time stabilizable. This completes the proof. ■

4.2. TSM disturbance observer design

In this subsection, a TSM disturbance observer is designed to estimate the system uncertainties.

Theorem 3. *Consider System (13), the TSM disturbance observer is designed as (26), (27), (29) and (33). With the tracking control law (15) and the compensating law (34), the closed-loop system finally evolves in a neighborhood around the origin.*

Proof. Consider System (13), take the control law as

$$u=u_{nom}+u_{com},\quad u_{com}=-\hat{G}, \tag{25}$$

where $\hat{G}$ represents the estimation of system uncertainties. If $u_{com}=-G$, then the effect of system uncertainties can be eliminated.

To design a TSM disturbance observer, an auxiliary sliding variable is introduced as [34,35]

$$\psi=x_2+\rho, \tag{26}$$

where ρ is designed as

$$\dot{\rho}=-u_{nom}. \tag{27}$$

Differentiating (26) with respect to time yields

$$\begin{aligned}\dot{\psi} &= \dot{x}_2 + \dot{\rho} \\ &= u_{nom} + u_{com} + G - u_{nom} \\ &= -\hat{G} + G. \end{aligned} \tag{28}$$

If $\hat{G}$ is chosen as

$$\hat{G} = \alpha_1 \psi + \alpha_2 \psi^k + \zeta \,\text{sign}(\psi), \tag{29}$$

where $0 < k < 1$, $\zeta > \bar{G}$, α_1 and α_2 are positive constants. Then the variable ψ converges to zero in finite time.

Define a Lyapunov function as

$$V_3 = \frac{1}{2}\psi^2. \tag{30}$$

Its derivative is

$$\begin{aligned}\dot{V}_3 &= \psi\dot{\psi} \\ &= \psi\left(G - \alpha_1\psi - \alpha_2\psi^k - \zeta \,\text{sign}(\psi)\right) \\ &\le \bar{G}\,|\psi| - \alpha_1\psi^2 - \alpha_2\psi^{k+1} - \zeta\,|\psi| \\ &\le -\alpha_1\psi^2 - \alpha_2\psi^{k+1} \\ &= -2\alpha_1 V_3 - \alpha_2\left(\sqrt{2}\right)^{k+1} V_3^{\frac{k+1}{2}}. \end{aligned} \tag{31}$$

According to Theorem 1, the variable ψ converges to zero in finite time. After $\dot{\psi} = 0$, the system uncertainties can be estimated by

$$G = \hat{G}_{eq}, \tag{32}$$

where $\hat{G}_{eq}$ denotes the average effect of the high-frequency switching control (29). It can be obtained by a low pass filter (LPF) which is implemented as [36,37]

$$\hat{G}'_{eq} = \frac{1}{\beta\ell + 1}\hat{G}, \quad \beta\dot{\hat{G}}'_{eq} = -\hat{G}'_{eq} + \hat{G}, \tag{33}$$

where ℓ is the differential operator and $\beta > 0$ is the time constant of the filter.

The output of LPF $\hat{G}'_{eq}$ can estimate $\hat{G}_{eq}$, and consequently the system uncertainty G asymptotically. The estimation error is proportional to the time constant β of LPF, $\left|\hat{G}'_{eq} - \hat{G}_{eq}\right| < o(\beta)$, then $\left|\hat{G}'_{eq} - G\right| < o(\beta)$. It is worth noting that β can be taken very small. Then, the convergence of (33) will be fast, and the estimation error will be very small.

The compensating law based on the TSM disturbance observer is

$$u_{com} = -\hat{G}'_{eq}. \tag{34}$$

With (34), System (13) is equivalent to

$$\begin{cases}\dot{x}_1 = x_2 \\ \dot{x}_2 = u_{nom} \pm o(\beta). \end{cases} \tag{35}$$

Through adjusting the parameters of (29), the variable ψ quickly converges to zero. With a small β, the estimation error $o(\beta)$ will be sufficiently small that the major impact of system uncertainties can be eliminated. According to Theorem 2, with (22), we obtain the following inequality

$$\begin{aligned}\dot{V}_2 \le &-\left(a - 2^{1-\frac{1}{q}}\right)x_1^d + \left(2^{1-\frac{1}{q}} + 2^{2-\frac{2}{q}}\frac{1}{a}\right)\varepsilon^d \\ &+ \frac{1}{\left(2-\frac{1}{q}\right)a^{1+q}}\varepsilon^{2-\frac{1}{q}}\left(u_{nom} \pm o(\beta)\right). \end{aligned} \tag{36}$$

Substituting u_{nom} in (15) into (36) yields

$$\begin{aligned}\dot{V}_2 &\le -\mu x_1^d - \mu\varepsilon^d \pm \frac{1}{\left(2-\frac{1}{q}\right)a^{1+q}}\varepsilon^{2-\frac{1}{q}}o(\beta) \\ &\le -\mu x_1^d - \mu\varepsilon^d + |\varepsilon|^{2-\frac{1}{q}}\,\vartheta(\beta) \\ &= -\mu x_1^d - \varepsilon^d\left(\mu - |\varepsilon|^{1-\frac{2}{q}}\,\vartheta(\beta)\right), \end{aligned} \tag{37}$$

where $\vartheta(\beta) = \frac{o(\beta)}{\left(2-\frac{1}{q}\right)a^{1+q}}$.

When $|\varepsilon| \ge \left(\frac{\vartheta(\beta)}{\mu}\right)^{\frac{q}{2-q}}$, it gives $\mu - |\varepsilon|^{1-\frac{2}{q}}\,\vartheta(\beta) > 0$, which implies that $\dot{V}_2 < 0$. So the convergence domain can be obtained as

$$\Pi: \ |\varepsilon| \le \left(\frac{\vartheta(\beta)}{\mu}\right)^{\frac{q}{2-q}} \tag{38}$$

where $\varepsilon = x_2^q + a^q x_1$.

Thus, the states of System (35) converge to a neighborhood around the origin.

This completes the proof. ■

4.3. Adaptive compensator design

In this subsection, an adaptive compensator is developed in the case that the upper boundary $\bar{G}$ is unknown.

Theorem 4. *Consider System (13), let the control input u be*

$$u = u_{nom} + u_{com}, \quad u_{com} = -\hat{G}\,sign(\sigma), \tag{39}$$

where u_{nom} is the tracking control law (15). The parameters of the compensating law u_{com} are taken as

$$\dot{\hat{G}} = |\sigma|, \quad \sigma = \frac{1}{\left(2-\frac{1}{q}\right)a^{1+q}}\varepsilon^{2-\frac{1}{q}},$$

$$sign(\sigma) = \begin{cases}1, & \sigma > 0 \\ 0, & \sigma = 0 \\ -1, & \sigma < 0. \end{cases}$$

Then, the control law (39) stabilizes System (13).

Proof. Let $\tilde{G} = \bar{G} - \hat{G}$, define a Lyapunov function for System (13) as

$$\begin{aligned}V_4 &= V_2 + \frac{1}{2}\tilde{G}^2 \\ &= \frac{1}{2}x_1^2 + \frac{1}{\left(2-\frac{1}{q}\right)a^{1+q}}\int_{x_2^*}^{x_2}\left(s^q - x_2^{*q}\right)^{2-\frac{1}{q}}ds + \frac{1}{2}\tilde{G}^2. \end{aligned} \tag{40}$$

Differentiating (40) with respect to time, from (21) and (22), we obtain

$$\begin{aligned}\dot{V}_4 \le &-\left(a - 2^{1-\frac{1}{q}}\right)x_1^d + \left(2^{1-\frac{1}{q}} + 2^{2-\frac{2}{q}}\frac{1}{a}\right)\varepsilon^d \\ &+ \frac{1}{\left(2-\frac{1}{q}\right)a^{1+q}}\varepsilon^{2-\frac{1}{q}}(u+G) - \tilde{G}\dot{\hat{G}}. \end{aligned} \tag{41}$$

Then, substituting (39) into (41) yields

$$\begin{aligned}\dot{V}_4 &\le -\mu x_1^d - \mu\varepsilon^d + \sigma(G - \hat{G}\,\text{sign}(\sigma)) - \tilde{G}\,|\sigma| \\ &\le -\mu x_1^d - \mu\varepsilon^d + \tilde{G}\,|\sigma| - \tilde{G}\,|\sigma| \\ &\le -\mu x_1^d - \mu\varepsilon^d. \end{aligned} \tag{42}$$

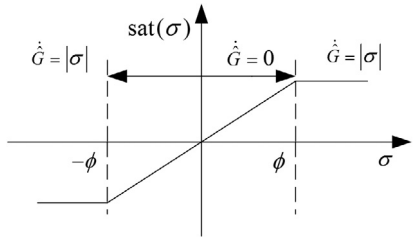

Fig. 3. Switching adaptive law.

According to the Lyapunov stability theory, the system states are asymptotically stable.

This completes the proof. ■

The switching function sign(·) in (39) leads to chattering. This is not desirable in control practice. A typical solution is the boundary layer approach that uses the saturation function sat(·) instead of sign(·). Note that there exists $|\sigma| \neq 0$ in the boundary layer. As the adaptive law $\dot{\hat{G}} = |\sigma|$ is an integrator, $\hat{G}$ grows unboundedly in the boundary layer. This is not accepted. Since this problem happens in the boundary layer, the most direct solution is to modify the adaptive law in the boundary layer. So, a switching adaptive law is presented in the following theorem.

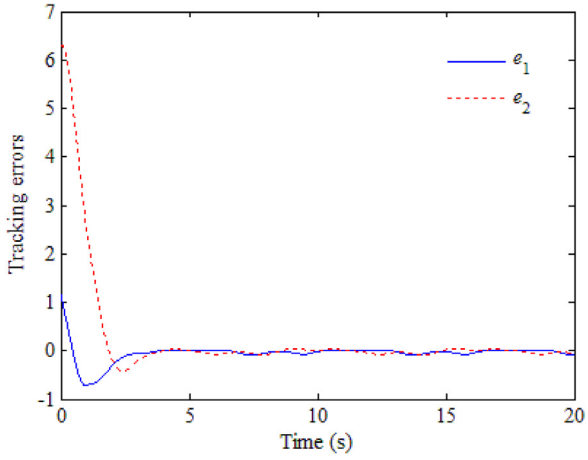

Fig. 5. Tracking errors (m) of u_{nom} (53) under uncertainties (52).

Theorem 5. *Consider System (13), and let the adaptive compensator u_{com} in (39) be*

$$u_{com} = -\hat{G}\, sat(\sigma)$$
$$\dot{\hat{G}} = \begin{cases} |\sigma|, & |\sigma| > \phi \\ 0, & |\sigma| \leq \phi, \end{cases} \qquad sat(\sigma) = \begin{cases} sign(\sigma), & |\sigma| > \phi \\ \sigma/\phi, & |\sigma| \leq \phi, \end{cases} \tag{43}$$

where ϕ is a positive constant.

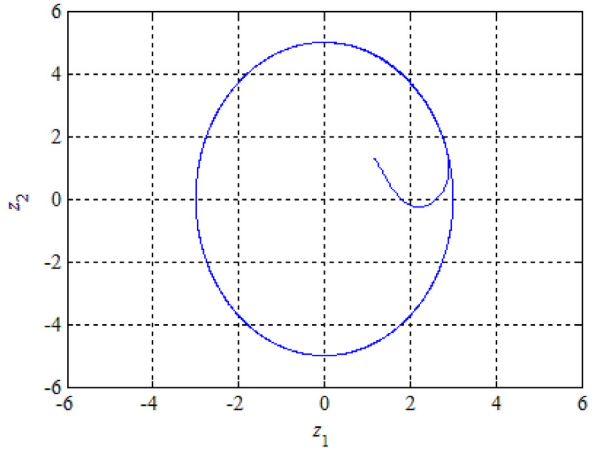

(a) Trajectory (m).

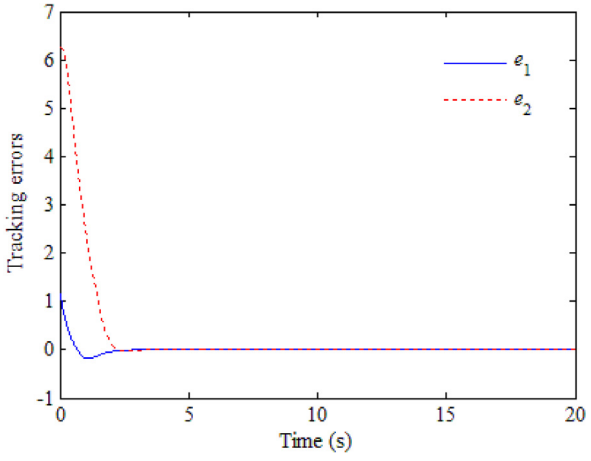

(b) Tracking errors (m).

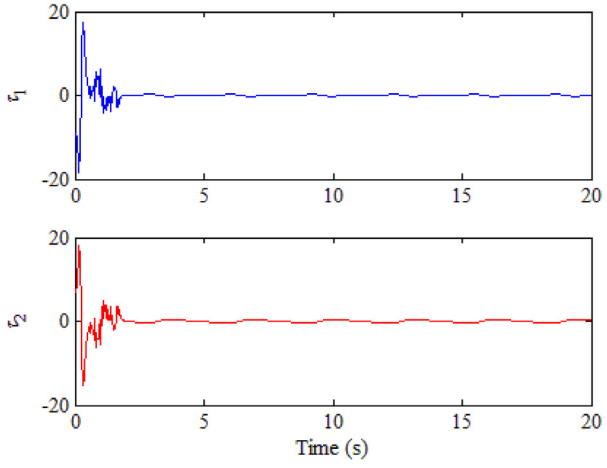

(c) Control torques (N m).

Fig. 4. Simulation result of nominal system with u_{nom} (53).

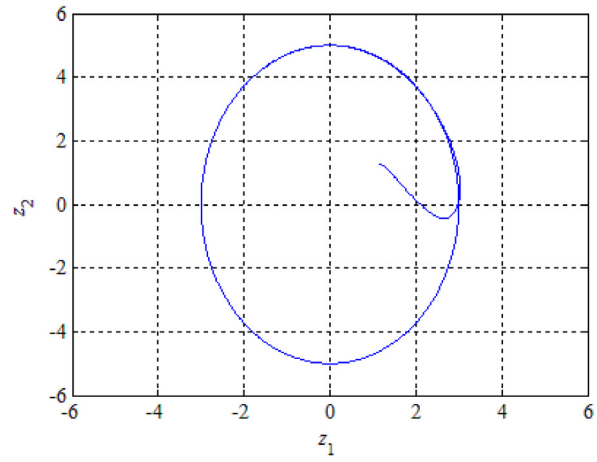

(a) Trajectory (m).

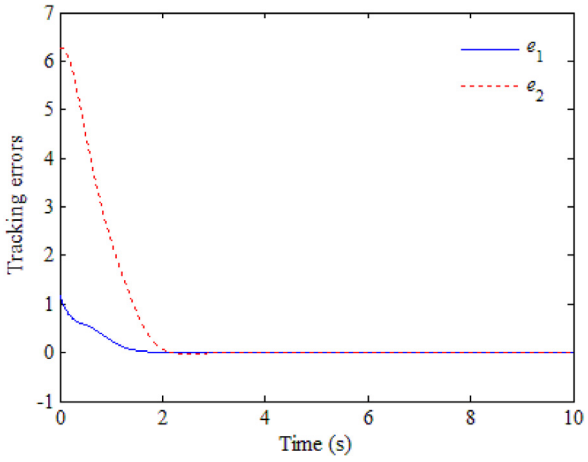

(b) Tracking errors (m).

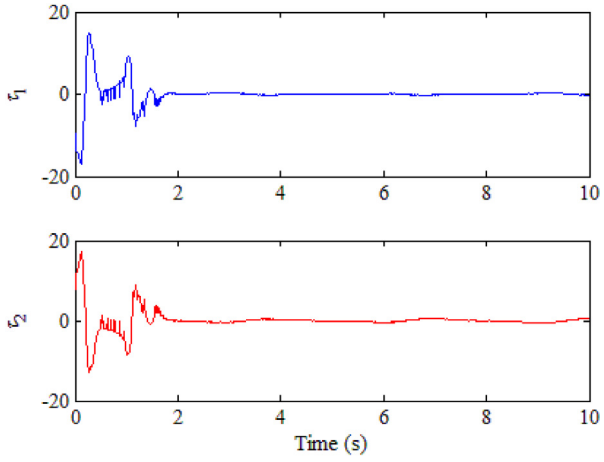

(c) Control torques (N m).

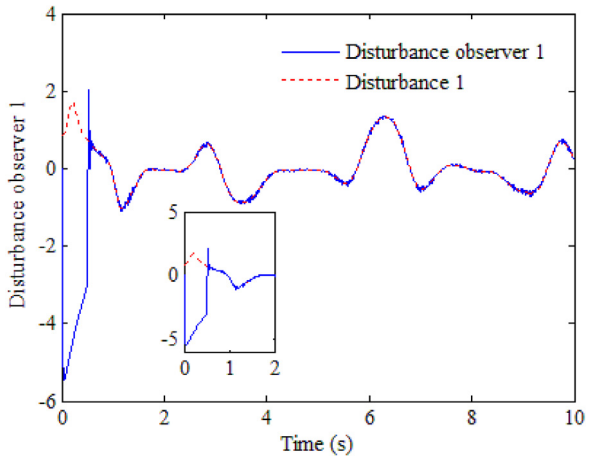

(d) Estimation of disturbance observer 1.

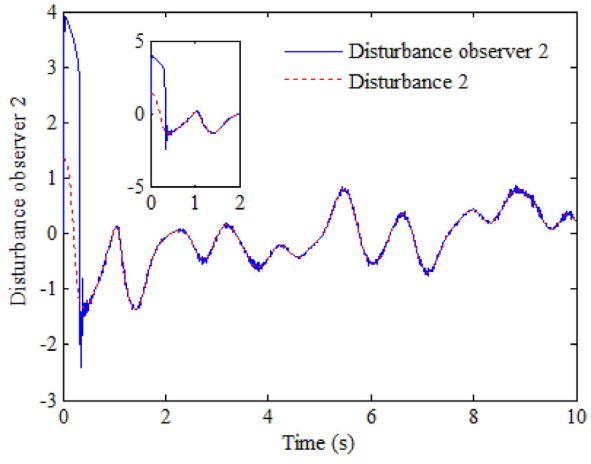

(e) Estimation of disturbance observer 2.

Fig. 6. Simulation result of u_{com} (55) under uncertainties (54).

Then, the ultimate boundedness of both the system states and the adaptive gain is guaranteed.

Proof. According to Theorem 4, it is easy to know that System (13) can be driven into the boundary layer, $|\sigma| \leq \phi$. The switching adaptive law (Fig. 3) ensures that the adaptive gain stops growing in the boundary layer.

If the stability of system states in the boundary layer is the only consideration, then, from (40) and (41), V_2 satisfies

$$\dot{V}_2 \leq -\left(a - 2^{1-\frac{1}{q}}\right) x_1^d + \left(2^{1-\frac{1}{q}} + 2^{2-\frac{2}{q}} \frac{1}{a}\right) \varepsilon^d + \frac{1}{\left(2-\frac{1}{q}\right) a^{1+q}} \varepsilon^{2-\frac{1}{q}} (u+G). \tag{44}$$

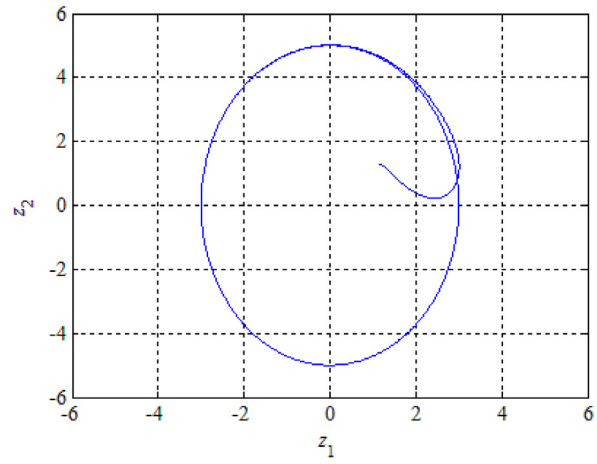

(a) Trajectory (m).

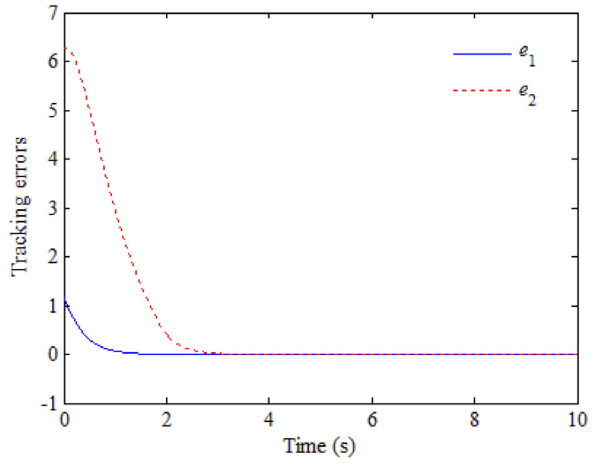

(b) Tracking errors (m).

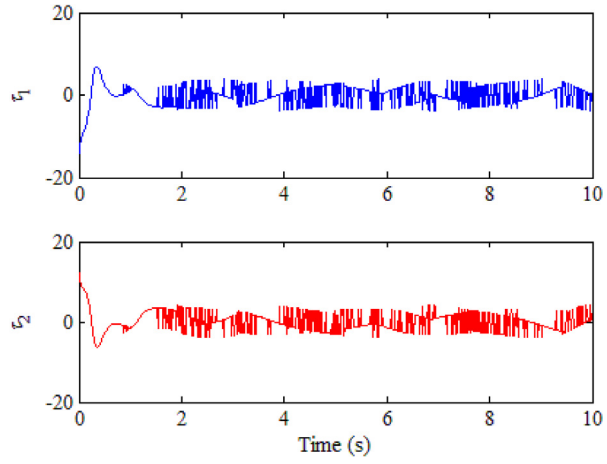

(c) Control torques (N m).

Fig. 7. Simulation result of LSM control law (56) under uncertainties (54).

Substituting u_{nom} in (15) and u_{com} in (43) into (44) yields

$$\dot{V}_2 \leq -\mu x_1^d - \mu\varepsilon^d + \sigma(G - \hat{G}\sigma/\phi). \tag{45}$$

If $\sigma\left(G - \hat{G}\sigma/\phi\right) \leq 0$, then $\sigma^2 - \frac{G\phi}{\hat{G}}\sigma \geq 0$. A conservative convergence domain of System (13) is

$$|\sigma| \leq \frac{\bar{G}\phi}{\hat{G}}. \tag{46}$$

If $\hat{G} < \bar{G}$, (46) shows that the convergence domain is larger than the boundary layer. It indicates that the state can escape from the boundary layer. According to (43), the adaptive compensator switches to the form, $u_{com} = -\hat{G}\,\mathrm{sign}(\sigma)$ and $\dot{\hat{G}} = |\sigma|$, outside the boundary layer. So $\hat{G}$ continues to grow. And the system state will converge into the boundary layer again. Then, the adaptive compensator switches to the form, $u_{com} = -\hat{G}\sigma/\phi$ and $\dot{\hat{G}} = 0$, in the boundary layer. At this moment, if $\hat{G}$ is still smaller than $\bar{G}$, (46) shows that the state can escape again. Finally, if $\hat{G}$ is equal to $\bar{G}$ or even larger than $\bar{G}$, (46) shows that the convergence domain is equal to or smaller than the boundary layer. Then, the escaping process cannot happen again. The system state will stay in the boundary layer, and $\hat{G}$ will stop growing. So, the ultimate boundedness of both the system states and adaptive gain is guaranteed.

The boundary of system states can be estimated in the boundary layer. According to Theorem 2, the parameters are chosen to be

$$\sigma = \frac{1}{\left(2 - \frac{1}{q}\right)a^{1+q}}\varepsilon^{2-\frac{1}{q}}, \quad \varepsilon = x_2^q - x_2^{*q},\ x_2^* = -ax_1^{\frac{1}{q}}, \tag{47}$$

where $1 < q < 2$. It can be rewritten as

$$x_2^q + a^q x_1 = \varepsilon, \quad \varepsilon = \left(\left(2 - \frac{1}{q}\right)a^{1+q}\sigma\right)^{\frac{q}{2q-1}}. \tag{48}$$

Since $|\sigma| \leq \phi$, we obtain $|\varepsilon| \leq \left(\left(2 - \frac{1}{q}\right)a^{1+q}\phi\right)^{\frac{q}{2q-1}}$.

In the case that $x_1x_2 \geq 0$, it yields $|a^q x_1| \leq |\varepsilon|$ and $\left|x_2^q\right| \leq |\varepsilon|$. So

$$|x_1| \leq \frac{|\varepsilon|}{a^q}, \qquad |x_2| \leq |\varepsilon|^{1/q}. \tag{49}$$

In the case that $x_1x_2 < 0$, it yields $x_1\dot{x}_1 < 0$ which implies that the domain of x_1 can be obtained by $\dot{x}_1 = 0$. With $x_2^q + a^q x_1 = \varepsilon$, we obtain

$$|x_1| \leq \frac{|\varepsilon|}{a^q}, \qquad |x_2| \leq |2\varepsilon|^{1/q}. \tag{50}$$

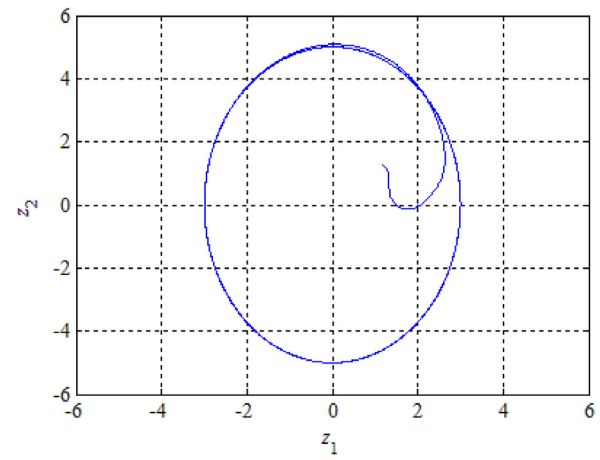

(a) Trajectory (m).

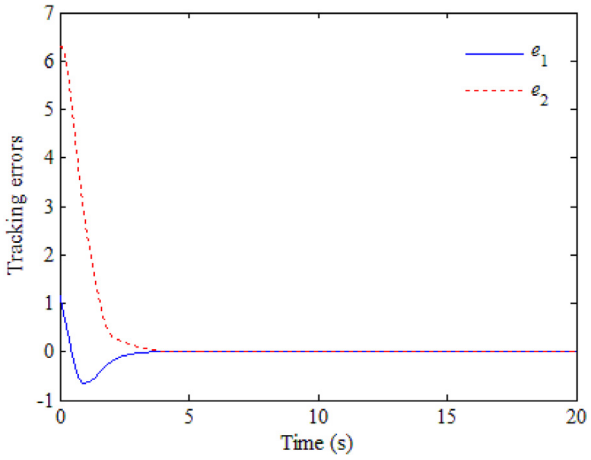

(b) Tracking errors (m).

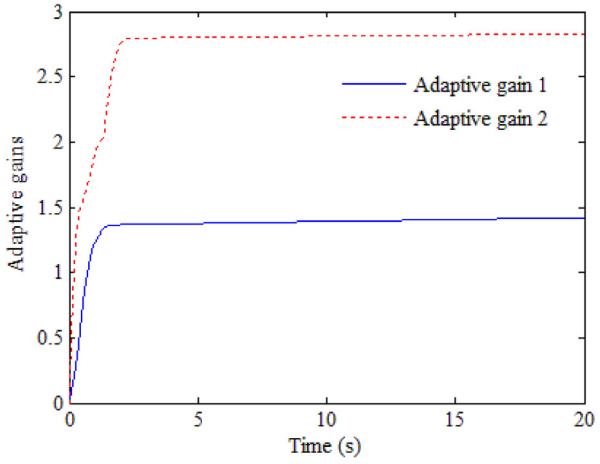

(c) Adaptive gains.

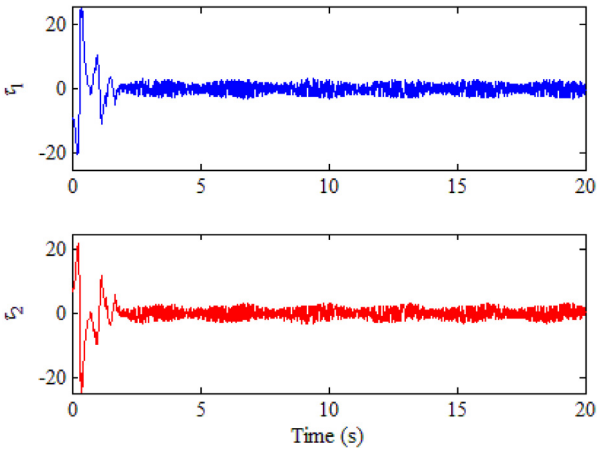

(d) Control torques (N m).

Fig. 8. Simulation result of adaptive compensator (57) under uncertainties (52).

Comparing (49) with (50), the boundary of system states can be estimated by

$$\Sigma: \quad |x_1| \le \frac{1}{a^q}\left(\left(2-\frac{1}{q}\right)a^{1+q}\phi\right)^{\frac{q}{2q-1}}, \qquad |x_2| \le 2^{1/q}\left(\left(2-\frac{1}{q}\right)a^{1+q}\phi\right)^{\frac{1}{2q-1}}. \tag{51}$$

This completes the proof. ■

5. Simulations

In this section, the control system design presented in Section 4 is verified by four steps. First, the tracking controller in Theorem 2 is checked. Second, the TSM disturbance observer is verified, and the proposed method in Theorem 3 is compared with the linear sliding mode (LSM) method of [16]. Then, the adaptive compensator is tested, and the proposed method in Theorem 4 is compared with the twisting algorithm (TA) method of [19]. Finally, the improved adaptive compensator in Theorem 5 is verified.

The structure parameters of a WMR are $m = 4$ kg, $R = 0.03$ m, $L = 0.15$ m, $I = 2.5$ kg m^2, and $h = 0.3$ m [19]. The reference trajectory is chosen as $z_{1d} = 3\sin(t)$ and $z_{2d} = -5\cos(t)$. The control input (15) needs to be transformed to the actual control torque through $\tau = A^{-1}(U - b)$. The tracking errors, e_1 and e_2, are those between Z and Z_d in (9).

The initial values were set to be $[x(0), y(0), \theta(0)]^{\mathrm{T}} = [1, 1, 1]$ and $[v(0), \omega(0)]^{\mathrm{T}} = [1, 1]$. The parameters in (15) were chosen to be $q = 13/11$ and $\mu = 0.2$. These give $a = 1.3125$ and $l = 4.9283$. The parameters in (29) and (33) were chosen to be $\alpha_1 = \alpha_2 = 1$, $k = 0.6$, $\zeta = 3$, and $\beta = 0.01$. The parameters for (39) and (43) were $\hat{G}(0) = [0, 0]^{\mathrm{T}}$ and $\phi = [0.05, 0.05]^{\mathrm{T}}$.

5.1. Tracking controller

In this subsection, the tracking control law is tested for both the nominal system and the uncertain system with changes of parameters and measurement noise (white Gaussian noise with Signal to Noise Ratio 50 dB).

Assume the parameter uncertainties were

$$\Delta R = 0.1R\sin(t), \qquad \Delta m = 0.4m, \qquad \Delta I = 0.3I\cos(t). \tag{52}$$

According to Theorem 2, we obtained the tracking control law as

$$u_{nom} = -4.9283\left(x_2^{\frac{13}{11}} - 1.379x_1\right)^{\frac{9}{13}}. \tag{53}$$

Fig. 4 Shows that the tracking controller (53) is effective for the nominal system. Tracking errors converged to zero in $t < 3.5$ s (Fig. 4(b)), and the control torques were chattering-free (Fig. 4(c)). On the other hand, when the plant has uncertainties, Fig. 5 shows that the tracking controller cannot handle the uncertainties.

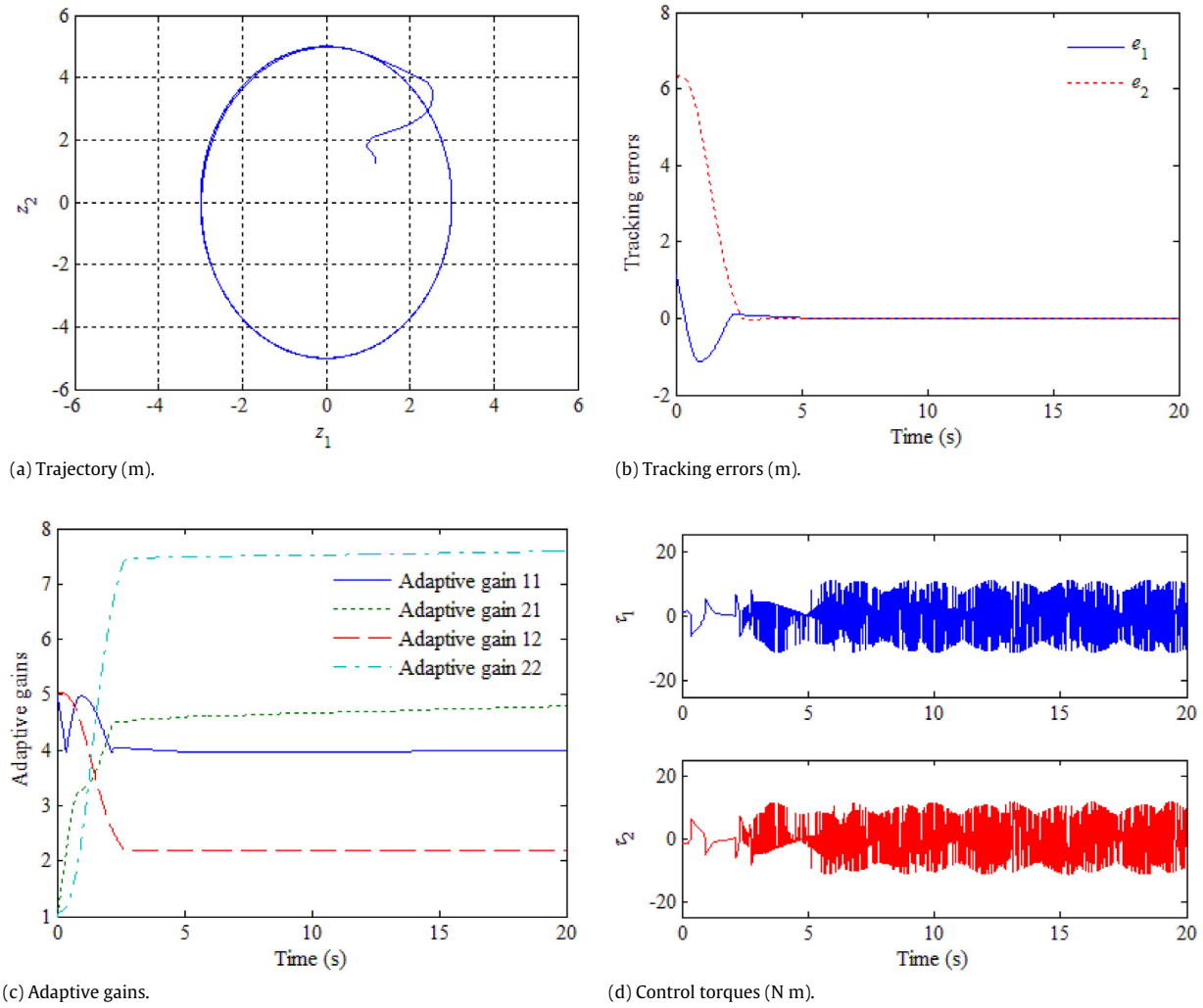

(a) Trajectory (m).

(b) Tracking errors (m).

(c) Adaptive gains.

(d) Control torques (N m).

Fig. 9. Simulation result of adaptive TA controller (58) under uncertainties (52).

Although the system was stabilized, the tracking errors converged into the range of ± 0.1 instead of zero.

5.2. TSM disturbance observer

In this subsection, the tracking control law (53) is cooperated with the TSM disturbance observer in Theorem 3. The measurement noise (white Gaussian noise with Signal to Noise Ratio 60 dB) is considered. And the external disturbances are taken as

$$\begin{aligned} \tau_{d1} &= 0.05 \sin(2\cos(3t)) + 0.03\cos(t), \\ \tau_{d2} &= 0.1 \sin(3\cos(1.5t)) + 0.1\cos(2\sin(t)). \end{aligned} \tag{54}$$

According to Theorem 3, we designed the compensating law as

$$\begin{aligned} u_{com} &= -\hat{G}_{eq}, \qquad \hat{G} = \psi + \psi^{0.6} + 3\text{sign}(\psi), \\ \dot{\hat{G}}_{eq} &= -100\hat{G}_{eq} + 100\hat{G}. \end{aligned} \tag{55}$$

In this subsection, the proposed method ((53) and (55)) is compared with the LSM control method of [16] as

$$u = -3x_2 - S - 3\,\text{sat}(S), \quad S = x_2 + 3x_1. \tag{56}$$

As shown in Fig. 6, the disturbance observer (55) had an accurate estimation of the external disturbances. The tracking errors decreased to zero in $t < 3.5$ s (Fig. 6(b)). From Fig. 6(d) and (e), it is clearly shown that the disturbance observers gave an accurate estimation in $t < 1$ s which was shorter than the convergence time of the tracking errors. Its fast estimation benefits from the fast convergence property of the TSM. Since the estimation errors are sufficiently small, the effect of system uncertainties can be eliminated. Thus, the convergence of tracking errors is guaranteed.

Fig. 7 Shows the simulation result of the LSM method. The tracking errors converged into to a small region of zero in $t < 4$ s (Fig. 7(b)). Even the boundary layer approach was used, the chattering in the control torques were obvious (Fig. 7(c)). Moreover, since the switching gain in (56) was a constant, the amplitude of control torques in Fig. 7(c) was high (± 4), whereas it varied in the range of ± 0.5 in Fig. 6(c).

Comparing Figs. 6 and 7 indicates that the proposed method in Theorem 3 cost less energy while it had better response. The advantage resulted from the fast accuracy estimation of the disturbance observer. Being different from the continuous constant compensating of the switching function, the disturbance observer gave an equivalent compensating for the external disturbances. So, the large conservative switching gain of the LSM method was avoided.

5.3. Adaptive compensator

In this subsection, the parameter uncertainties (52) and measurement noise (with Signal to Noise Ratio 45 dB) are considered. The tracking controller (53) is cooperated with the

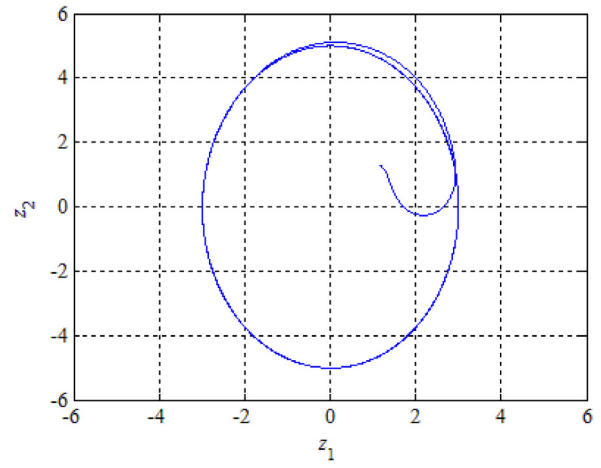

(a) Trajectory (m).

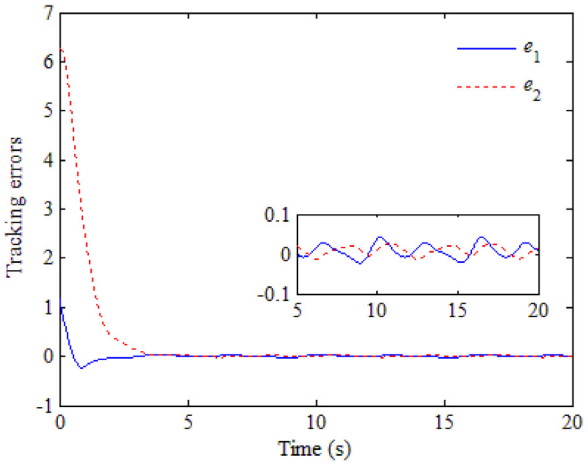

(b) Tracking errors (m).

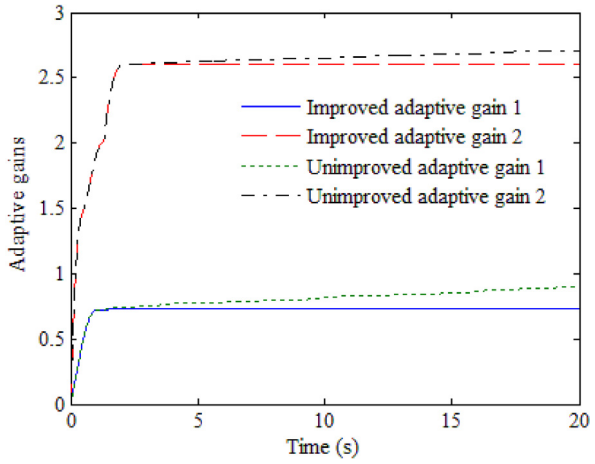

(c) Adaptive gains.

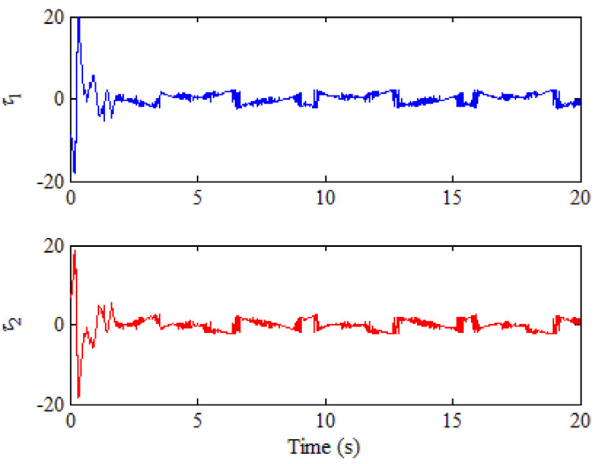

(d) Control torques (N m).

Fig. 10. Simulation result of improved adaptive compensator (59) under uncertainties (60).

following adaptive compensator

$$u_{com} = -\hat{G}\,\mathrm{sign}\left(0.4788\left(x_2^{\frac{13}{11}} - 1.379x_1\right)^{\frac{15}{13}}\right). \tag{57}$$

Here, the proposed method ((53) and (57)) is compared with the adaptive TA method in [19] as

$$\begin{aligned} &u = -\hat{r}_1\,\mathrm{sign}(x_1) - \hat{r}_2\,\mathrm{sign}(x_2)\\ &\dot{\hat{r}}_1 = k_1 x_2\,\mathrm{sign}(x_1), \qquad \dot{\hat{r}}_2 = k_2\,|x_2|\\ &\hat{r}_1(0) = \begin{bmatrix}5\\5\end{bmatrix}, \qquad \hat{r}_2(0) = \begin{bmatrix}1\\1\end{bmatrix},\\ &k_1 = \begin{bmatrix}0.9\\0.45\end{bmatrix}, \qquad k_2 = \begin{bmatrix}1\\1\end{bmatrix}. \end{aligned} \tag{58}$$

As shown in Fig. 8, the adaptive compensator (57) handled the uncertainties effectively. The tracking errors decreased to zero in Fig. 8(b). The adaptive gains adjusted automatically under the unknown uncertainties (Fig. 8(c)). The chattering in the control torques occurred due to the switching function in the adaptive compensator (Fig. 8(d)).

Fig. 9 Shows the simulation results of the adaptive TA method. The tracking errors decreased to zero in Fig. 9(b), which cost 1.5 s longer than that in Fig. 8(b). The adaptive gains adjusted automatically (Fig. 9(c)), and there was also chattering in the control torques (Fig. 9(d)). The control torques varied in the range of ±12, whereas it was ±4 in Fig. 8(d).

Comparing Figs. 8 and 9 indicates that the proposed method is more efficient. In addition, there are two switching functions with different variables in the adaptive TA controller. It is difficult to give a solution for reducing chattering and guaranteeing the boundedness of adaptive gains simultaneously. So, the proposed method is more suitable for actual applications.

5.4. Improved adaptive compensator

In order to attenuate the chattering in the control torque, the adaptive compensator (57) is improved by combination of the boundary layer approach and a switching adaptive law. According to (43) in Theorem 5, we obtained

$$u_{com} = -\hat{G}\mathrm{sat}\left(0.4788\left(x_2^{\frac{13}{11}} - 1.379x_1\right)^{\frac{15}{13}}\right). \tag{59}$$

As shown in Fig. 3, the switching function is substituted by a linear function in the boundary layer. When the tracking errors converge into the boundary layer, the amplitudes of control torques become smaller and change slower than that outside the boundary layer. As a result, the chattering is reduced. However, the nonzero states inside the boundary layer result in the unboundedly growing of the adaptive gain. Therefore, a switching adaptive law is introduced in (43).

In this subsection, the validity of improved adaptive compensator (59) is tested by the measurement noise (with Signal to Noise Ratio 50 dB) and the following system uncertainties

$$\begin{aligned} &\tau_{d1} = 0.1\sin(t), \qquad \tau_{d2} = 0.1\cos(t) \\ &\Delta R = 0.15R\sin(t), \qquad \Delta m = 0.2\,m, \qquad \Delta I = 0.1I\cos(t). \end{aligned} \tag{60}$$

Clearly in Fig. 10(b), the steady-state (take $t \geq 5$ s) tracking errors converged into the range of ± 0.05, which satisfied the estimated boundary ± 0.1023 given by (51). Fig. 10(c) show that the improved adaptive gains converged to constants, $\hat{G}_1 = 0.73$ and $\hat{G}_2 = 2.6$. It verified that the adaptive gains stopped growing when the errors converged into the boundary layer. On contrast, the unimproved adaptive gains grew unboundedly. Comparing Fig. 8(d) and Fig. 10(d) shows that the chattering in the control torques was attenuated.

5.5. Discussions of the control method

The above simulation results have confirmed the validity of the proposed control method. Furthermore, the scope and limitation of the control method should be noted.

First, the boundary information of system uncertainties is a parameter in the design of disturbance observer. The disturbance observer cannot be applied in the case that the boundary information of system uncertainties is unknown.

Second, the adaptive compensator is effective for complex system uncertainties, such as the external disturbances, the changes of parameters, and measurement noise. For the asymptotical convergence of the adaptive compensator, the closed-loop control system is asymptotically stable instead of finite-time stable. The chattering in the adaptive compensator is suppressed at the sacrifice of tracking accuracy. So the tracking error converges to the vicinity of zero rather than zero. Moreover, because of the continuous constant compensating of the adaptive compensator, it has larger amplitude than the disturbance observer.

6. Conclusion

In this paper, the robust trajectory tracking control for a WMR was investigated. The designed tracking controller provided finite-time convergence of the tracking errors for the nominal plant, the disturbance observer and adaptive compensator enhanced the robustness of the control system against system uncertainties. The simulation results confirmed that the presented control method was effective. By comparing with the existing control methods (LSM and TA), the presented control method showed better performance.

Acknowledgment

This research is supported by National Natural Science Foundation of China (No. 61375100, No. 61433003, and No. 61472037).

References

[1] Francisco G. Rossomando, Carlos Soria, Ricardo Carelli, Sliding mode neuro adaptive control in trajectory tracking for mobile robots, J. Intell. Robot. Syst. 74 (3–4) (2014) 931–944.
[2] Yunjeong Kim, Byung Kook Kim, Efficient time-optimal two-corner trajectory planning algorithm for differential-driven wheeled mobile robots with bounded motor control inputs, Robot. Auton. Syst. 64 (2015) 35–43.
[3] I. Kanellakopoulos, P.V. Kokotovic, Systematic design of adaptive controllers for feedback linearizable systems, IEEE Trans. Automat. Control 36 (11) (1991) 1241–1253.
[4] V.I. Utkin, Variable structure systems with sliding modes, IEEE Trans. Automat. Control 22 (2) (1977) 212–222.
[5] Arie Levant, Principles of 2-sliding mode design, Automatica 43 (4) (2007) 576–586.
[6] Yong Feng, Xinghuo Yu, Zhihong Man, Non-singular terminal sliding mode control of rigid manipulators, Automatica 38 (12) (2002) 2159–2167.
[7] Sanjay P. Bhat, Dennis S. Bernstein, Finite-time stability of homogeneous systems, in: Proceedings of the American Control Conference, 4, 1997, pp. 2513–2514.
[8] W.Q. Tang, Y.L. Cai, High-order sliding mode control design based on adaptive terminal sliding mode, Internat. J. Robust Nonlinear Control 23 (2) (2013) 149–166.
[9] Zhongping Jiang, Henk Nijmeijer, Tracking control of mobile robots: A case study in backstepping, Automatica 33 (7) (1997) 1393–1399.
[10] Ti Chung Lee, Kai Tai Song, Ching Hung Lee, Ching Cheng Teng, Tracking control of unicycle-modeled mobile robots using a saturation feedback controller, IEEE Trans. Control Syst. Technol. 9 (2) (2001) 305–318.
[11] Takanori Fukao, Hiroshi Nakagawa, Norihiko Adachi, Adaptive tracking control of a nonholonomic mobile robot, IEEE Trans. Robot. Autom. 16 (5) (2000) 609–615.
[12] C.K. Li, Hongmin Chao, Y.M. Hu, A.B. Rad, Output tracking control of mobile robots based on adaptive backstepping and high order sliding modes, in: 2002 IEEE International Conference on Systems, Man and Cybernetics, 2002, 4 (5), pp. 135–138.
[13] Dongkyoung Chwa, Fuzzy adaptive tracking control of wheeled mobile robots with state-dependent kinematic and dynamic disturbances, IEEE Trans. Fuzzy Syst. 20 (3) (2012) 587–593.
[14] Jung Min Yang, Jong Hwan Kim, Sliding mode control for trajectory tracking of nonholonomic wheeled mobile robots, IEEE Trans. Robot. Autom. 15 (3) (1999) 578–587.
[15] Dongkyoung Chwa, Sliding-mode tracking control of nonholonomic wheeled mobile robots in polar coordinates, IEEE Trans. Control Syst. Technol. 12 (4) (2004) 637–644.
[16] Razvan Solea, Adrian Filipescu, Urbano Nunes, Sliding mode control for trajectory tracking of a wheeled mobile robot in presence of uncertainties, in: Proceedings of 7th Asia Control Conference, 2009, pp. 1701–1706.
[17] Chih Yang Chen, Tzuu Hseng S. Li, Ying Chieh Yeh, Cha Cheng Chang, Design and implementation of an adaptive sliding mode dynamic controller for wheeled mobile robots, Mechatronics 19 (2) (2009) 156–166.
[18] Meiying Ou, Haibo Du, Shihua Li, Finite-time tracking control of multiple nonholonomic mobile robots, J. Franklin Inst. B 349 (9) (2012) 2834–2860.
[19] Jie Yang, Qinglin Wang, Yuan Li, An improved second order sliding mode twisting algorithm for finite-time trajectory tracking of intelligent vehicle, Adv. Mech. Eng. (2013) 1–8.
[20] Yihong Zhao, Jiping Zhou, Rongfa Chen, A terminal sliding mode tracking control algorithm for mobile robots, Key Eng. Mater. 375–376 (2008) 588–592.
[21] Ahmed S. Al-Araji, Maysam F. Abbod, Hamed S. Al-Raweshidy, Applying posture identifier in designing an adaptive nonlinear predictive controller for nonholonomic mobile robot, Neurocomputing 99 (2013) 543–554.
[22] Ming Yue, Shuang Wang, Yongshun Zhang, Adaptive fuzzy logic-based sliding mode control for a nonholonomic mobile robot in the presence of dynamic uncertainties, J. Mech. Eng. Sci. 229 (11) (2015) 1979–1988.
[23] Fang Yang, Chaoli Wang, Adaptive tracking control for uncertain dynamic nonholonomic mobile robots based on visual servoing, J. Control Theory Appl. 10 (1) (2012) 56–63.
[24] J. Chen, W.E. Dixon, D.M. Dawson, M. McIntyre, Homography-based visual servo tracking control of a wheeled mobile robot, IEEE Trans. Robot. 22 (2) (2006) 407–416.
[25] Zhongxu Hu, Yueming Hu, Zongyuan Mao, Robust output tracking control based on the dynamical model of nonholonomic mobile robots, Control Decis. 15 (5) (2000) 599–601.
[26] Hyun-Sik Shim, Hyun-Sik Shim, Asymptotic control for wheeled mobile robots with driftless constraints, Robot. Auton. Syst. 43 (2003) 29–37.
[27] Sašo Blažič, A novel trajectory-tracking control law for wheeled mobile robots, Robot. Auton. Syst. 59 (2011) 1001–1007.
[28] Graham Wheeler, Chun Yi Su, Yury Stepanenko, A sliding mode controller with improved adaptation laws for the upper bounds on the norm of uncertainties, Automatica 34 (12) (1998) 1657–1661.
[29] Zhihong Man, O'Day Mike, A robust adaptive terminal sliding mode control for rigid robotic manipulators, J. Intell. Robot. Syst. 24 (1) (1999) 23–41.
[30] Xianqing Huang, Wei Lin, Bo Yang, Global finite-time stabilization of a class of uncertain nonlinear system, Automatica 41 (5) (2005) 881–888.
[31] Shihua Li, Shihong Ding, Yuping Tian, A finite-time state feedback stabilization method for a class of second order nonlinear systems, Acta Automat. Sinica 33 (1) (2007) 101–104.
[32] Shihong Ding, Shihua Li, Qi Li, Stability analysis for a second-order continuous finite-time control system subject to a disturbance, J. Control Theory Appl. 7 (3) (2009) 271–276.
[33] Shuanghe Yu, Xinghuo Yu, Bijan Shirinzadeh, Zhihong Man, Continuous finite-time control for robotic manipulators with terminal sliding mode, Automatica 41 (11) (2005) 1957–1964.
[34] Peng Li, Zhiqiang Zheng, Jianjun Ma, Global robust finite time stabilization of a class of nonlinear uncertain systems, Control Theory Appl. 28 (7) (2011) 915–920.
[35] Mou Chen, Qing-Xian Wu, Rong-Xin Cui, Terminal sliding mode tracking control of a class of SISO uncertain nonlinear systems, ISA Trans. 52 (2) (2013) 198–206.
[36] Jin Li, Liu Yang, Finite-time terminal sliding mode tracking control for piezoelectric actuators, Abstr. Appl. Anal. (2014) 1–9.
[37] Charles E. Hall, Yuri B. Shtessel, Sliding mode disturbance observer-based control for a reusable launch vehicle, J. Guid. Control Dyn. 29 (6) (2006) 1315–1328.

Linjie Xin received the B.S. degree in electrical engineering from Yantai University, Yantai, China, in 2008 and the M.S. degree in control engineering from Zhengzhou University of Light Industry, Zhengzhou, China, in 2012. He is currently working toward the Ph.D. degree in the School of Automation, Beijing Institute of Technology, Beijing, China.

His current research interests include adaptive, finite-time control of nonlinear systems, and mobile robotics.

Qinglin Wang received the B.S. degree in control science and engineering from Beijing Institute of Technology, Beijing, China, in 1983 and the Ph.D. degree in control science and engineering from Chinese Academy of Science, Beijing, in 1998.

In 1990, he joined the School of Automation, Beijing Institute of Technology, where he is currently a professor. His research interests include equilibrium state control theory, control of mobile robotics, and nonlinear control. Dr. Wang is a member of Chinese Association of Automation (CAA).

Jinhua She received the B.S. degree in engineering from Central South University, Changsha, China, in 1983, and the M.S. and Ph.D. degrees in engineering from the Tokyo Institute of Technology, Tokyo, Japan, in 1990 and 1993, respectively.

He joined the staff of School of Computer Science, Tokyo University of Technology in 1993, where he is currently a professor. His current research interests are repetitive control, nonlinear control, robust control, and robotics. Dr. She is a member of the Society of Instrument and Control Engineers (SICE), the Institute of Electrical Engineers of Japan (IEEJ), the Japan Society of Mechanical Engineers (JSME), and the Asian Control Association (ACA). He received the International Federation of Automatic Control (IFAC) Control Engineering Practice Paper Prize in 1999 (jointly with M. Wu and M. Nakano).

Yuan Li received the B.S. and M.S. degrees in electrical engineering from Dalian Jiaotong University, Dalian, China, in 1999 and 2002, respectively, and the Ph.D. degree in control science and engineering from Chinese Academy of Science, Beijing, China, in 2006.

In 2006, he joined Beijing Institute of Technology, Beijing. He was a Senior Researcher Associate from September 2007 to January 2008 in the City University of Hong Kong, Kowloon, Hong Kong. His research interests include robotics and computer vision, particularly visual measurement and control of robots.